

Manganese-Catalyzed Hydroboration of Terminal Olefins and Metal-Dependent Selectivity in Internal Olefin Isomerization–Hydroboration

Subhash Garhwal,[†] Asja A. Kroeger,[†] Ranjeesh Thenarukandiyil, Natalia Fridman, Amir Karton,^{*} and Graham de Ruiter^{*}

Cite This: <https://dx.doi.org/10.1021/acs.inorgchem.0c03451>

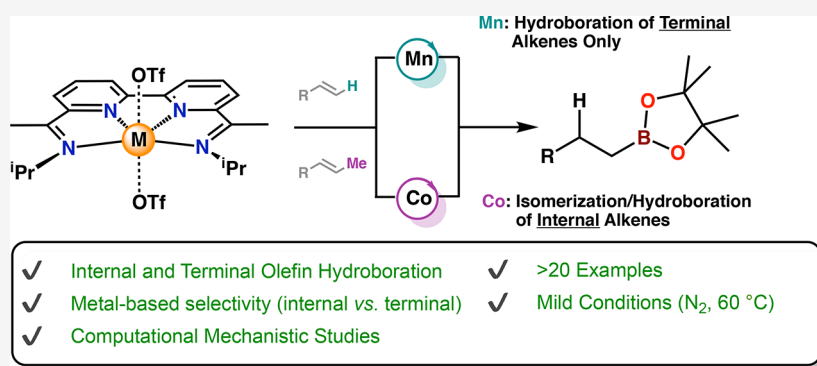
Read Online

ACCESS |

Metrics & More

Article Recommendations

Supporting Information



ABSTRACT: In the past decade, the use of earth-abundant metals in homogeneous catalysis has flourished. In particular, metals such as cobalt and iron have been used extensively in reductive transformations including hydrogenation, hydroboration, and hydrosilylation. Manganese, on the other hand, has been considerably less explored in these reductive transformations. Here, we report a well-defined manganese complex, [Mn(^{Pr}Bdi)(OTf)₂] (**2a**; Bdi = bipyridinediimine), that is an active precatalyst in the hydroboration of a variety of electronically differentiated alkenes (>20 examples). The hydroboration is specifically selective for terminal alkenes and occurs with exclusive anti-Markovnikov selectivity. In contrast, when using the analogous cobalt complex [Co(^{Pr}Bdi)(OTf)₂] (**3a**), internal alkenes are hydroborated efficiently, where a sequence of isomerization steps ultimately leads to their hydroboration. The contrasting terminal versus internal alkene selectivity for manganese and cobalt was investigated computationally and is further discussed in the herein-reported study.

INTRODUCTION

The continuous effort to present a more sustainable outlook for future generations has led to a renaissance in the use of earth-abundant metals in homogeneous catalysis.¹ Their natural abundance, low toxicity, and ready availability have been strong incentives to replace their less environmentally friendly noble-metal counterparts. Furthermore, the smaller ionic radii and typically high-spin electronic structures of earth-abundant metals have resulted in a unique reactivity that can be otherwise hard to realize with their heavier congeners.² The success of earth-abundant metals results not only from their unique reactivity in different spin states³ but also from their ability to engage in reliable two-electron chemistry via metal–ligand cooperativity.⁴ As a result, during the past few years, earth-abundant metals have extensively been utilized as catalysts in many organic transformations.^{5,6}

From among the earth-abundant metals such as manganese, iron, and cobalt, catalysts that are based on iron and cobalt

have received much attention in recent years.⁷ In contrast, reductive transformations with manganese have been under-represented in the literature.⁸ Typically, manganese-mediated transformations are reported for manganese(I), which avoids the unfavorable high-spin ($S = 5/2$) configuration of manganese(II).^{9,10} Indeed, the groups of Milstein,¹¹ Kempe,¹² Beller,¹³ Kirchner,¹⁴ and others¹⁵ have demonstrated that manganese(I) can be an effective catalyst in several organic transformations.⁸ Yet, the application of manganese in the hydroboration of alkenes has rarely been reported.¹⁶

Received: November 23, 2020

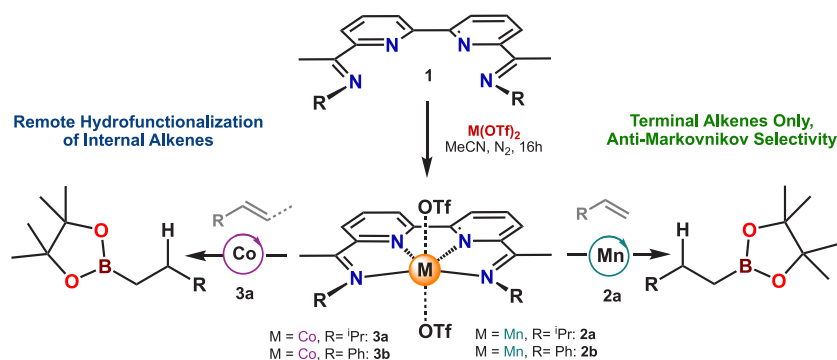


Figure 1. Metal-dependent (manganese versus cobalt) selectivity in the hydroboration of terminal and internal alkenes, leading to their isomerization/hydrofunctionalization with cobalt.

The hydroboration of alkenes is an effective and atom-economic method for generating alkylboronate esters, which are versatile reagents in many organic transformations,¹⁷ particularly in metal-mediated cross-coupling reactions.¹⁸ Traditionally, catalytic alkene hydroboration has been catalyzed by precious metals such as rhodium, ruthenium, and iridium.¹⁹ At present, alkene hydroboration with earth-abundant metals such as cobalt,²⁰ iron,²¹ nickel,²² and copper²³ is well established,²⁴ while for manganese, only a few reports have appeared in the recent literature.¹⁶

To better understand the differences between manganese and cobalt in the hydroboration of alkenes and to expand the limited use of manganese in this useful transformation, we prepared isostructural complexes $[\text{Mn}(\text{PrBDI})(\text{OTf})_2]$ (**2a**; BDI = bipyridinediimine) and $[\text{Co}(\text{PrBDI})(\text{OTf})_2]$ (**3a**). As we will demonstrate, the manganese complex **2a** is an active precatalyst for the hydroboration of terminal alkenes. The hydroboration occurs with exclusive anti-Markovnikov regioselectivity (Figure 1) and with good functional group tolerance in both linear olefins and styrenes. When the metal center is changed from manganese (**2a**) to cobalt (**3a**), the reactivity toward internal alkenes can be turned on, resulting in their isomerization–hydroboration (Figure 1), which is a topic of much current interest.²⁵ The observed metal-based divergence between manganese and cobalt was investigated computationally, suggesting that the metal-dependent selectivity results from olefin migratory insertion into the metal hydride, which is more favorable for cobalt than for manganese. Furthermore, the effect of the spin state was also investigated, revealing that high-spin manganese(II) complexes can be beneficial for catalysis.

RESULTS AND DISCUSSION

Synthesis of Manganese and Cobalt Metal Complexes. We commenced our studies by synthesizing the corresponding manganese and cobalt complexes **2a** and **3a**. Stirring an acetonitrile solution of the BDI ligand with an anhydrous metal triflate salt resulted in the clean formation of complexes **2a** and **3a**. The ¹H NMR spectra of **2a** and **3a** only show (broad) proton resonances between −20 and 150 ppm, consistent with the formation of paramagnetic species (Figures S15 and S19). However, their high-resolution mass spectrometry spectra are consistent with the formation of **2a** and **3a**. We note that, on the basis of ¹⁹F NMR spectroscopy, it is highly likely that the triflates in complexes **2a** and **3a** are not bound to the metal center in solution.

Structural details for complexes **2a** and **3a** were obtained by X-ray crystallographic studies on crystals formed via the slow vapor diffusion of diethyl ether into a concentrated solution of **2a** or **3a** in acetonitrile (Figure 2). Both complexes are similar

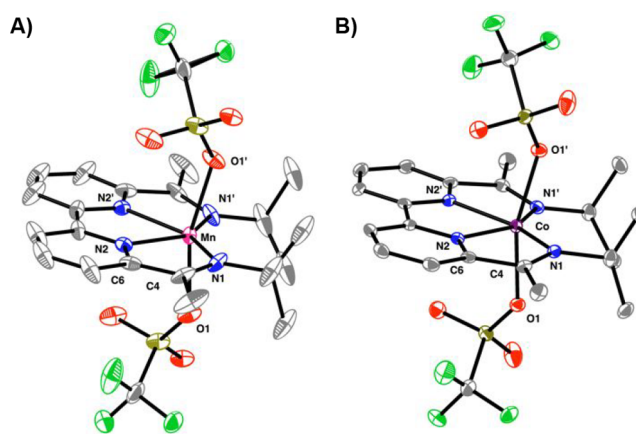


Figure 2. Solid-state structures of (A) **2a** and (B) **3a**. Thermal ellipsoids are shown at the 30% probability level. Hydrogen atoms and cocrystallized solvent molecules are omitted for clarity.

in structure, with two axially bound triflates and the four nitrogen atoms of the BDI ligand (N1–N4) in the equatorial plane. On the basis of charge balance, the manganese and cobalt metal centers are assigned as manganese(II) and cobalt(II), respectively. The average $C_{\text{imine}}\text{--}N_{\text{imine}}$ distances of 1.282(7) Å (**2a**) and 1.281(4) Å (**3a**) and the average $C_{\text{ipso}}\text{--}C_{\text{imine}}$ distances of 1.480(8) Å (**2a**) and 1.499(4) Å (**3a**) are also indicative of an M(II) (M = metal) center that is supported by a neutral BDI ligand (Table S2).²⁶

The paramagnetic nature of complexes **2a** and **3a** was further confirmed by SQUID magnetometry via temperature-dependent analysis of the magnetic moment (Figure 3). For the manganese complex **2a**, the magnetic moment is nearly temperature-independent between 300 and 6 K ($\mu_{\text{eff}} = 6.05\text{--}6.11$) and decreases below 6 K to 5.72 (Figure 3, red trace). The room temperature value of $\mu_{\text{eff}} = 6.05$ is close to the expected spin-only value of 5.92 for an $S = 5/2$ system, consistent with an assignment of $[\text{Mn}^{\text{II}}(\text{BDI})^0(\text{OTf})_2]$ containing a high-spin Mn^{II} d^5 metal center.²⁷ For cobalt, the room temperature value of the magnetic moment of $\mu_{\text{eff}} = 4.82$ (**3a**) is higher than the spin-only value of 3.87 expected for a spin $3/2$ system, but deviation is commonly observed for high-spin Co^{II} d^7 metal complexes.^{27d,28} Below 130 K, the

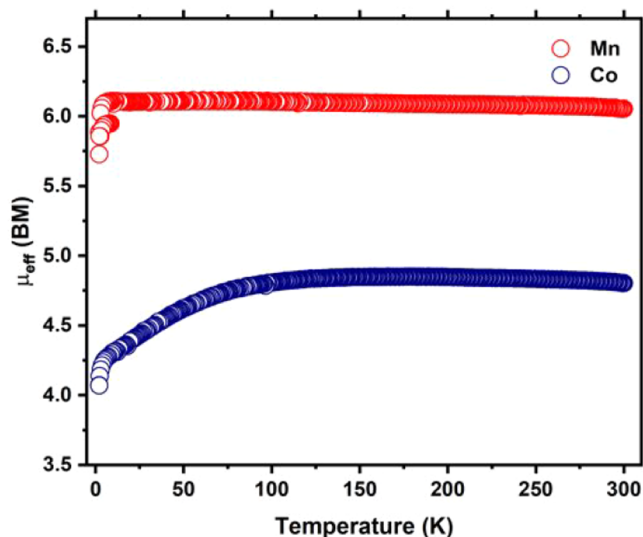


Figure 3. Temperature dependence of the effective magnetic moment (μ_{eff}) for complexes **2a** (red circles) and **3a** (blue circles).

magnetic moment gradually decreases to a value of $\mu_{\text{eff}} = 4.07$ at 2K, most probably because of weak intermolecular antiferromagnetic interactions at low temperature (Figure 3, blue trace).

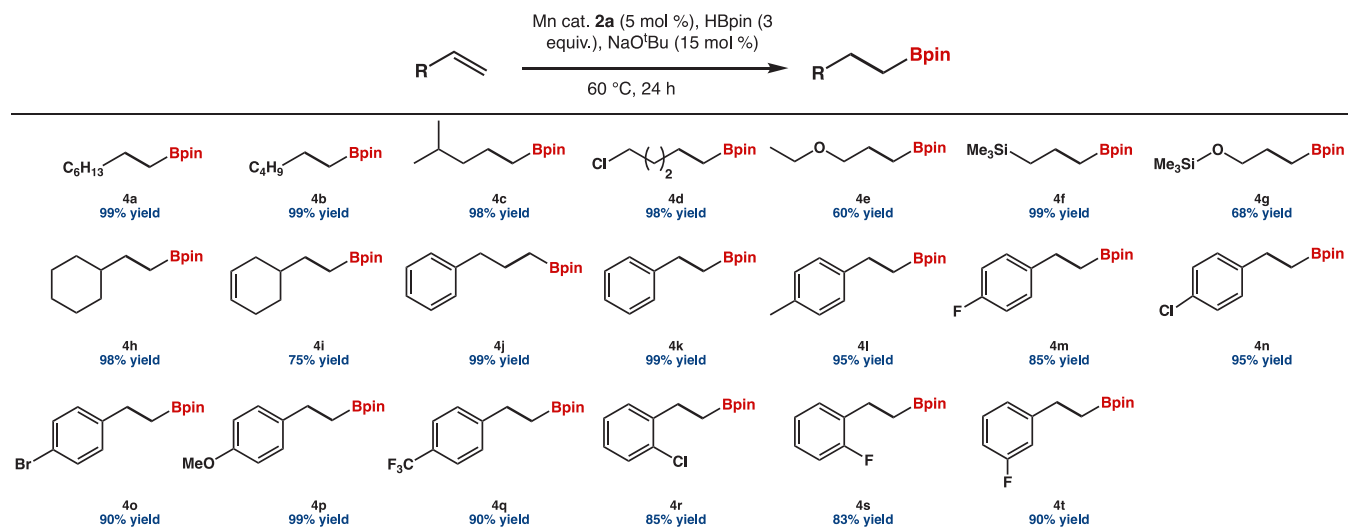
Catalytic Hydroboration. With complexes **2a** and **3a** in hand, we explored their initial reactivity in the hydroboration of unactivated alkenes. The hydroboration of alkenes is an important reaction that gives facile access to alkylboronate esters frequently used as intermediates in the fine chemical industry. Using complex **2a** (5 mol %), in the presence of pinacolborane (HBpin; 3 equiv) with NaO^tBu (15 mol %) as the activator,²⁹ 1-hexene was selectively converted to the corresponding terminal alkylboronate ester. The reaction occurs under mild conditions (60 °C, N₂) and typically takes 24 h to reach complete conversion. Under these conditions, further investigation into the substrate scope demonstrates that

2a hydroborates a variety of alkenes with excellent yields (>99%) and with exclusive anti-Markovnikov regioselectivity (Table 1). The functional group tolerance includes halogens (**4d**), ethers (**4e** and **4g**), internal alkenes (**4i**), and silyl substituents (**4f**), although the (silyl)ether substituent in **4g** does give somewhat of a diminished yields (Table 1; 60–70%). Aside from linear alkenes, various electronically and sterically differentiated styrenes are also borylated with high efficiency and regioselectivity. For example, para-substituted styrenes bearing electron-withdrawing (e.g., –F, –Cl, –Br, or –CF₃) or electron-donating (e.g., –OMe or –Me) substituents are hydroborated with excellent yields (85–99%) and with exclusive anti-Markovnikov regioselectivity (Table 1; entries **4l–4q**). Changing the substitution pattern from para to either ortho or meta affects neither the yield nor the regioselectivity of the reaction (Table 1; entries **4r–4t**). These results demonstrate that the manganese complex **2a** is an effective precatalyst for the hydroboration of a wide variety of substituted alkenes, with observed anti-Markovnikov regioselectivities (>98%) that are comparable to the *state-of-the-art* for manganese.^{16a,b}

Recently, there has been considerable interest in alkene isomerization/hydrofunctionalization of olefins.²⁵ In this context, several studies have shown that cobalt complexes are good catalysts for this synthetically useful transformation.^{20d,n,o,q} We thus envisioned that changing the metal center from manganese (**2a**) to cobalt (**3a**) might give us access to this highly useful reaction via the selective isomerization of internal alkenes.^{16c}

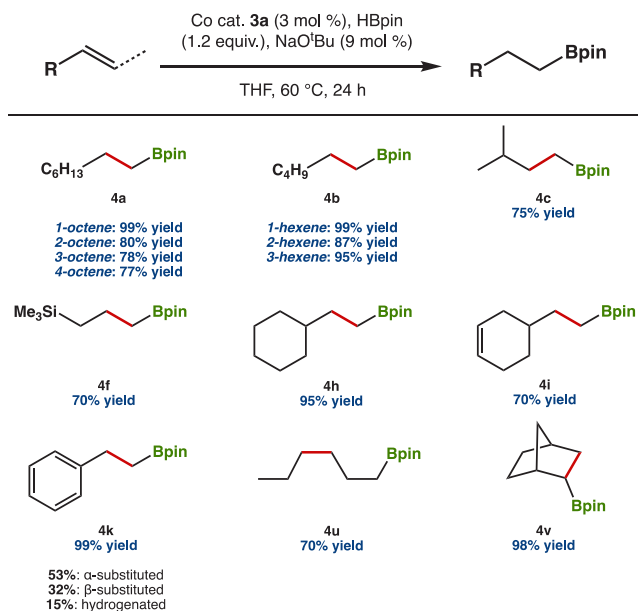
Using catalytic conditions similar to those for manganese (Table 1), we explored the activity of the cobalt complex **3a** in the hydroboration of alkenes (Table 2). To our delight, the cobalt catalyst **3a** affords good yields and exclusive anti-Markovnikov selectivity in the hydroboration of terminal alkenes. (Table 2, **4a–4c**, **4f**, **4h**, and **4i**). Styrene, on the other hand, gives a mixture of α - and β -substituted products, with a fair degree of hydrogenation of the double bond (Table 2; **4k**). The results obtained for **3a** and styrene are in direct contrast to

Table 1. Substrate Scope of the Manganese-Catalyzed (**2a**) Hydroboration of Terminal Alkenes^a



^aReactions were performed with alkene (0.5 mmol), HBpin (1.5 mmol, 3.0 equiv), NaO^tBu (0.075 mmol, 15 mol %), and catalyst **2a** (5 mol %) at 60 °C for 24 h (Table 1). Yields were determined by ¹H NMR spectroscopy in the presence of an internal standard. In all substrates, hydroboration occurs with almost exclusive anti-Markovnikov regioselectivity ($\geq 98\%$).

Table 2. Substrate Scope of the Cobalt-Catalyzed (3a) Hydroboration of Terminal Alkenes^a



^aReactions were performed with alkene (0.5 mmol), HBpin (0.6 mmol, 1.2 equiv), NaO^tBu (0.045 mmol, 9 mol %), and catalyst 3a (2 mol %) in tetrahydrofuran (0.5 mL) at 60 °C for 24 h (Table 1). Yields were determined by ¹H NMR spectroscopy in the presence of an internal standard. In all substrates, the hydroboration occurs with almost exclusive anti-Markovnikov regioselectivity ($\geq 98\%$).

the observed regioselectivity with 2a, which exclusively gives the linear β -substituted (anti-Markovnikov) borylation product (vide supra). An additional difference between 2a and 3a is that while the manganese catalyst 2a does not show any reactivity toward internal alkenes, 3a efficiently borylates internal alkenes to produce the terminal alkylboronate esters in good yields (Table 2). The hydroboration of internal alkenes occurs irrespective of the position of the double bond (Table 2, e.g., 4a; 2-octene vs 4-octene), although shorter alkenes are generally borylated more efficiently than longer ones (Table 2; compare 4a with 4b). Aside from the position of the double bond, their geometry is also important. For example, when using *cis*-3-hexene, yields are lower than those for *trans*-3-hexene (compare 4b and 4u). The observed terminal anti-Markovnikov borylation most likely occurs via consecutive alkene insertion and β -hydride elimination steps, providing a convenient method for alkene isomerization–hydroboration.²⁴ Indeed, isotope-labeling experiments are consistent with consecutive insertion/elimination steps (Figures S5–S8). The marked differences in selectivity with cobalt and manganese highlight the importance of the metal center in either (i) enabling β -hydride elimination necessary for alkene isomerization or (ii) their ability to generate a secondary metal–alkyl species upon insertion of the internal alkene into the M–H bond.

Before the origin of the difference in reactivity between 2a and 3a is discussed in more detail, it is important to note that, recently, it was reported that, under the experimental reaction conditions, the combination NaO^tBu/HBpin generates a good hydroboration catalyst (BH₃).³⁰ Notwithstanding, we believe that in this study complexes 2a and 3a are the active precatalysts based on the following observations: (i) for the cobalt-catalyzed hydroboration of styrene, product selectivities

different from those for borane are observed (Table 2; 4k);³⁰ (ii) for both cobalt and manganese, the hydroboration is sensitive toward modification of the imine substituent on the ligand (Figure 1), indicating a strong catalyst dependence (Table S1); (iii) the addition of TMEDA does not lead to complete inhibition of the observed catalysis (Figure S67).

Computational Mechanistic Investigations. In order to gain insights into the origins of the experimentally observed selectivity differences between complexes 2a and 3a, we subsequently studied the mechanism of the hydroboration reaction using density functional theory (DFT) methods. Hereby, we took into consideration the possibility of different spin states in the modeled complexes and the possibility for reversible metal–ligand coordination of the imine substituents (Tables S7–S12).³¹ Such structural flexibility has been previously observed by Solan and co-workers in related complexes with nickel and zinc.³²

To guide the computational studies, we first defined a plausible reaction mechanism that is based on literature precedent (Figure 4). The catalytic cycle starts with the

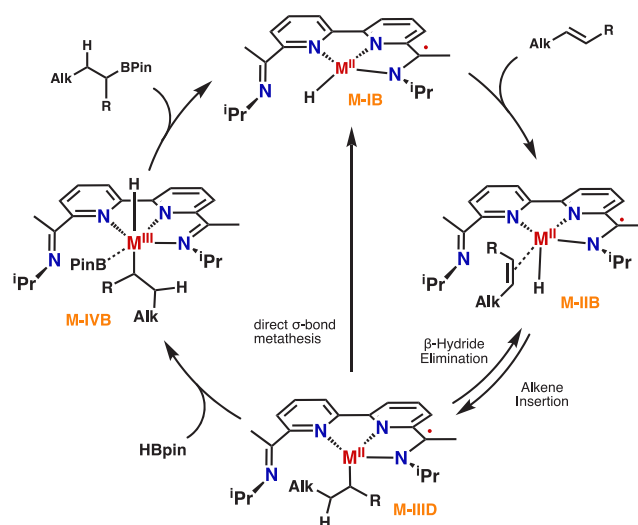


Figure 4. Plausible mechanism for the manganese- and cobalt-catalyzed hydroboration of alkenes.

formation of a metal hydride that is generated upon activation of the precatalyst with NaO^tBu and HBpin.²⁹ The importance of metal hydride intermediates in alkene hydroboration has also been demonstrated by Chirik,^{20q} Turculet,^{16c} and others.²⁴ Coordination of the alkene and subsequent insertion into the metal hydride generates a metal alkyl species. Finally, borylation can occur either via a stepwise oxidative addition/reductive elimination pathway or via a concerted σ -bond metathesis pathway (Figure 4). The validity of the proposed mechanism was investigated for both cobalt and manganese in order to unravel the origin of the observed selectivity differences for internal and terminal alkenes (vide infra). As we will demonstrate, decoordination of one of the ligand side arms herein is crucial in order to provide a vacant coordination site.

Cobalt-Catalyzed Olefin Hydroboration. Because complex 3a was able to efficiently catalyze the hydroboration of both terminal and internal alkenes, we will first discuss the computed mechanistic aspects of the cobalt-catalyzed hydroboration (Tables S9, S10, and S12). Hereafter, we will contrast the calculated mechanism with that calculated for manganese

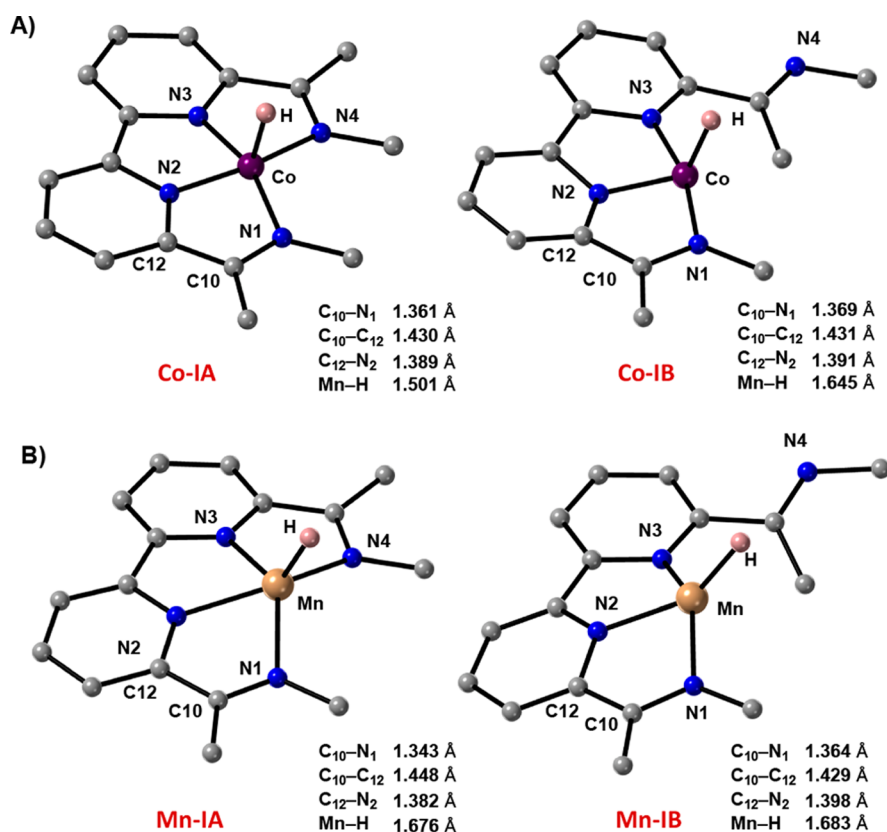


Figure 5. Calculated equilibrium structures for the corresponding cobalt (A) and manganese (B) hydrides in the singlet (cobalt) and quintet (manganese) states.

and explain the differences, leading to the observed selectivity for terminal and internal alkenes (vide infra).

For cobalt, hydroboration is initiated by formation of the corresponding hydride (Figure 4). The calculated geometries of the five- and four-coordinate cobalt hydride species **Co-IA** and **Co-IB** are shown in Figure 5A and feature a cobalt metal center in square-pyramidal and distorted “butterfly” geometries, respectively. For all cobalt complexes, the singlet, triplet, and quintet spin states were considered (Tables 3 and S9). Our calculations indicate that, for **Co-IA**, the singlet state is 15.1 kcal mol^{−1} lower in energy than the triplet state, while for **Co-IB**, the singlet and triplet states are nearly equal in energy (Table 3).³³ The calculated singlet state implies that the electronic structure features either (i) a genuine Co^I metal

center or (ii) a low-spin cobalt(II) metal center that is antiferromagnetically coupled to a ligand-based radical. Because the activation protocol and reaction conditions provide an overall reducing environment, redox noninnocence of the BDI ligand should not be ruled out.^{26a,34}

Analysis of the calculated geometry of **Co-IA** reveals that the N_{imine}–C_{imine} and C_{imine}–C_{ipso} bond lengths of 1.361 and 1.430 Å are indicative of a ligand-based radical, which necessitates a low-spin Co^{II} d⁷ metal center in **Co-IA**. Our calculations also indicate that, for hydroboration to proceed, ligand dissociation is necessary (Figures 4 and 6). Ligand dissociation from **Co-IA** to give **Co-IB** is energetically uphill by 25.1 kcal mol^{−1} and does not have a marked effect on the calculated bond distances (Table 3 and Figure 5). After formation of the cobalt hydride **Co-IB**, olefin coordination is exergonic by 1.8 kcal mol^{−1} (**Co-IIB**) on the singlet potential energy surface (PES; Figure 6 and Table S9). Migratory insertion of the olefin into the Co–H bond occurs with an overall barrier of 25.5 kcal mol^{−1} (TS1) and provides the secondary cobalt alkyl species **Co-IIIB**. The small activation energy (2.2 kcal mol^{−1}) required to transition from **Co-IIB** to **Co-IIIB** indicates that migratory insertion readily occurs once a single imine-ligand dissociates. A similar trend is observed for the triplet PES (Figure 6, blue trace). However, the overall energy barrier of 35.1 kcal mol^{−1} is significantly higher than that calculated for the singlet PES (25.5 kcal mol^{−1}). Hereafter, isomerization of the internal cobalt alkyl species **Co-IIIB** to the terminal cobalt alkyl species **Co-IIID** occurs via a sequence of β-hydride elimination and migratory insertion steps (Figure 6) with activation energies between 4 and 6 kcal mol^{−1}. Overall, there is very little thermodynamic preference for the internal versus terminal

Table 3. Relative Energies for Different Spin States of the Cobalt and Manganese Metal Hydrides upon Coordination (IA) and Decoordination (IB) of One of the Imine Side Arms

Spin state	Energy (kcal mol ^{−1})	
	Co-IA	Mn-IA
Singlet	0.0	25.5
Triplet	15.1	−2.3
Quintet		0.0
Spin state	Energy (kcal mol ^{−1})	
	Co-IB	Mn-IB
Singlet	25.1	50.6
Triplet	24.5	19.3
Quintet		12.9

Manganese-Catalyzed Olefin Hydroboration. Computational studies regarding the alkene hydroboration with manganese were initiated by evaluating the different spin-states for the manganese hydride complexes **Mn-IA** and **Mn-IB**. As is evident from Table 5, both the triplet and quintet spin

Table 5. Calculated Gibbs Free Energy (ΔG_{298} , kcal mol⁻¹) for the Migratory Insertion of 2-Butene^a

Complex	Energy (kcal mol ⁻¹)	
	Triplet	Quintet
Mn-IA	-2.3	0.0
Mn-IB	19.3	12.9
Mn-IIB	19.3	18.3
TSI	34.5	34.2
Mn-IIIB	25.2	7.3

^aFor computational details, see the Supporting Information.

states are close in energy ($\Delta\Delta G_{298} = 2.3$ kcal mol⁻¹); however, upon ligand decooordination, the quintet state is clearly preferred (Table 5).³⁵ The quintet spin state implies a high-spin Mn^{II} d⁵ metal center that is antiferromagnetically coupled to a ligand-based radical. The difference with the analogous cobalt complex is that, whereas **Co-IB** is low-spin, **Mn-IB** is high-spin. Aside from the differences in the favored spin states, there are no distinct structural differences between the cobalt and manganese hydride complexes **M-IA** and **M-IIB**, which is also reflected by their similar geometries and bond lengths.

In order to be able to explain the experimentally observed selectivity of the manganese catalyst **2a** for terminal alkenes, we begin by considering the mechanism and energetics of the migratory insertion of 2-butene (Tables 5 and S7). As is evident from Table 5, the computational results show that, on both the triplet and quintet PESs, the migratory insertion has a high activation energy of 34.5 and 34.2 kcal mol⁻¹, respectively (Table 5; **TS1**). On the other hand, the migratory insertion of 1-butene into the Mn–H bond has an activation energy that is lower by almost 3.0 kcal mol⁻¹ (Figure 7 and Table S8). Nonetheless, the energy barrier remains high and qualitatively explains why for manganese the hydroboration of terminal alkenes remains challenging. A survey across the reported manganese-catalyzed hydroboration reactions reveals that most of them require higher temperatures and longer reaction times, especially when compared to cobalt.^{16c,36}

Having explored the manganese-catalyzed alkene migratory insertion, we turn to the subsequent borylation step. First, we note that, because complex **2a** did not show any reactivity toward internal alkenes, the mechanistic aspects of their borylation will not be discussed. Notwithstanding, a full PES for the hydroboration of 2-butene is provided in Figure S75.

For the borylation of terminal manganese alkyl species **Mn-IIID**, calculations show that the lowest-energy pathway lies on the quintet PES (Tables 6 and S11). The borylation proceeds via a concerted σ -bond metathesis pathway with an activation energy of 20.5 kcal mol⁻¹. In contrast, on the triplet PES, borylation occurs via a stepwise oxidative addition–reductive elimination pathway with an energy barrier of 30.8 kcal mol⁻¹ (Table 6). Because the energy barrier for σ -bond metathesis is much lower than that calculated for migratory insertion (31.5 kcal mol⁻¹; Figure 7), migratory insertion is rate-limiting in the manganese-catalyzed hydroboration.

Upon comparison of these computational results with those obtained for cobalt, a few differences are noted. First, the rate-

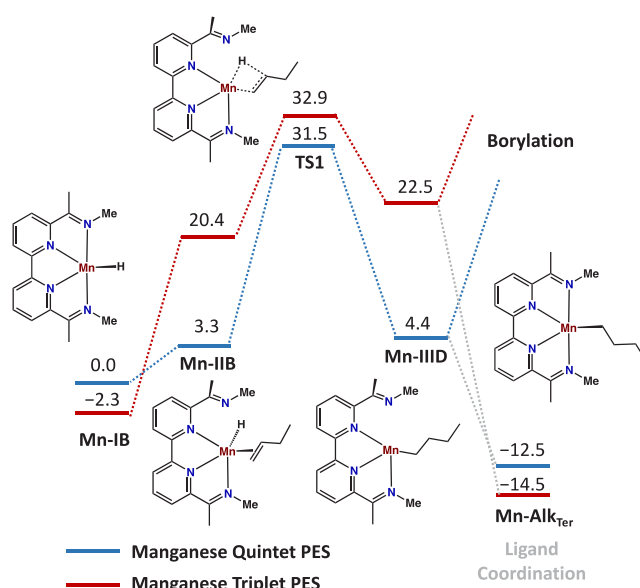


Figure 7. Calculated Gibbs free PES (ΔG_{298} , kcal mol⁻¹) for the hydroboration of 1-butene with complex **2a** with a triplet (red trace) or quintet (blue trace) spin state. For computational details, see the Supporting Information.

Table 6. Calculated Gibbs Free Energies (ΔG_{298} , kcal mol⁻¹) for the Borylation of Terminal Manganese Alkyl Species **Mn-IIID**^{a,b}

Complex	Energy (kcal mol ⁻¹)	
	Triplet	Quintet ^b
Mn-IIID	22.5	4.4
TS4_{Ox}	30.8	
Mn-IVD	12.8	
TSS_{Red} (or TS_{σ-bond})	31.2	20.5
Mn-V	12.8	3.2

^aFor computational details, see the Supporting Information.

^bCalculations indicate a direct σ -bond metathesis pathway.

limiting step for cobalt is the borylation via σ -bond metathesis, while for manganese, it is the migratory insertion of the alkene (Table 4 and Figure 7). The energy difference between the transition structures of the rate-limiting steps for cobalt (27.9 kcal mol⁻¹) and manganese (31.5 kcal mol⁻¹) indicates that the hydroboration of terminal alkenes should be more facile for cobalt than for manganese. These computational results are in qualitative agreement with the experimentally obtained results (Table S2). Under identical reaction conditions (60 °C, 3 mol % catalyst, and 1.2 equiv of HBpin), the cobalt catalyst **3a** converts 1-octene into the corresponding alkylboronate ester in 99% yield, while for the manganese catalyst **2a**, only 25% yield was observed. These observations are in line with other reported examples that demonstrate that, for manganese catalysis, typically higher temperatures and longer reaction times are required.^{16c,36}

Second, the herein-presented computational studies also point toward a difference in regioselectivity between manganese and cobalt complexes **2a** and **3a**. In particular, the computational results show that the manganese-catalyzed migratory insertion of an internal alkene is unlikely (34.2 kcal mol⁻¹), while for cobalt, there is no clear difference between the migratory insertion of an internal (25.5 kcal mol⁻¹) or a terminal (24.4 kcal mol⁻¹) alkene. This explains why, in

experiments, the cobalt complex **3a** is able to catalyze the hydroboration of both internal and terminal alkenes, while the manganese catalyst **2a** is selective for only terminal alkenes.

SUMMARY AND CONCLUSIONS

In summary, we have demonstrated that complexes of the types **2a** and **3a** are effective precatalysts for the hydroboration of terminal alkenes. The hydroboration reaction occurs under mild conditions (60 °C, N₂) and proceeds with exclusive anti-Markovnikov selectivity. When using internal alkenes, however, marked differences in the reactivities of the manganese and cobalt catalysts were observed. Whereas for manganese no reactivity was observed for internal alkenes, the cobalt complex **3a** was able to perform a tandem alkene isomerization/hydroboration reaction. To understand these differences in the reactivities, the reaction mechanism of the hydroboration reaction was investigated computationally, taking into consideration the different spin states and structural flexibilities of complexes **2a** and **3a**. We demonstrate that the observed metal-based divergence is due to differences in the energy barriers toward the initial migratory insertion of the internal alkene, which is much higher for manganese (34.2 kcal mol⁻¹) than for cobalt (25.5 kcal mol⁻¹).

ASSOCIATED CONTENT

Supporting Information

The Supporting Information is available free of charge at <https://pubs.acs.org/doi/10.1021/acs.inorgchem.0c03451>.

Synthetic procedures, characterization data, catalysis, and computational data (PDF)

Accession Codes

CCDC 2027374–2027377 contain the supplementary crystallographic data for this paper. These data can be obtained free of charge via www.ccdc.cam.ac.uk/data_request/cif, or by emailing data_request@ccdc.cam.ac.uk, or by contacting The Cambridge Crystallographic Data Centre, 12 Union Road, Cambridge CB2 1EZ, UK; fax: +44 1223 336033.

AUTHOR INFORMATION

Corresponding Authors

Amir Karton – School of Molecular Sciences, The University of Western Australia, 6009 Perth, WA, Australia; orcid.org/0000-0002-7981-508X; Email: amir.karton@uwa.edu.au

Graham de Ruiter – Schulich Faculty of Chemistry, Technion-Israel Institute of Technology, Technion City 3200008, Haifa, Israel; orcid.org/0000-0001-6008-286X; Email: graham@technion.ac.il

Authors

Subhash Garhwal – Schulich Faculty of Chemistry, Technion-Israel Institute of Technology, Technion City 3200008, Haifa, Israel; orcid.org/0000-0002-0093-9224

Asja A. Kroeger – School of Molecular Sciences, The University of Western Australia, 6009 Perth, WA, Australia; orcid.org/0000-0001-7699-541X

Ranjeesh Thenarukandiyil – Schulich Faculty of Chemistry, Technion-Israel Institute of Technology, Technion City 3200008, Haifa, Israel

Natalia Fridman – Schulich Faculty of Chemistry, Technion-Israel Institute of Technology, Technion City 3200008, Haifa, Israel

Complete contact information is available at:

<https://pubs.acs.org/10.1021/acs.inorgchem.0c03451>

Author Contributions

[†]S.G. and A.A.K. contributed equally.

Notes

The authors declare no competing financial interest.

ACKNOWLEDGMENTS

This research was supported by the Azrieli Foundation (Israel) and the Technion EVPR Fund–Mallat Family Research Fund. G.de.R. is an Azrieli young faculty fellow and a Horev Fellow supported by the Taub Foundation. R.T. thanks the Council for Higher Education in Israel for an incoming PBC fellowship. A.K. acknowledges resources from the National Computational Infrastructure, supported by the Australian Government, and system administration support provided by the Faculty of Science at the University of Western Australia to the Linux cluster of the Karton group. A.K. and A.A.K. gratefully acknowledge the provision of a Forrest Research Foundation Scholarship and an Australian Government Research Training Program Stipend (to A.A.K.) and an Australian Research Council Future Fellowship (to A.K.; Project FT170100373).

REFERENCES

- (1) Gebbink, R. J. M. K.; Moret, M. E. *Non-Noble Metal Catalysis: Molecular Approaches and Reactions*, 1st ed.; Wiley-VCH: Weinheim, Germany, 2019.
- (2) (a) Hu, M.; Ge, S. Versatile Cobalt-Catalyzed Regioselective Chain-Walking Double Hydroboration of 1,N-Dienes to Access Gem-Bis(Boryl)Alkanes. *Nat. Commun.* **2020**, *11*, 765. (b) Zhou, Y.-Y.; Uyeda, C. Catalytic Reductive [4 + 1]-Cycloadditions of Vinylidenes and Dienes. *Science* **2019**, *363*, 857. (c) Tondreau, A. M.; Atienza, C. C. H.; Weller, K. J.; Nye, S. A.; Lewis, K. M.; Delis, J. G. P.; Chirik, P. J. Iron Catalysts for Selective Anti-Markovnikov Alkene Hydro-silylation Using Tertiary Silanes. *Science (Washington, DC, U. S.)* **2012**, *335*, 567–570.
- (3) (a) Holland, P. L. Reaction: Opportunities for Sustainable Catalysts. *Chem.* **2017**, *2*, 443–444. (b) Holland, P. L. Distinctive Reaction Pathways at Base Metals in High-Spin Organometallic Catalysts. *Acc. Chem. Res.* **2015**, *48*, 1696–1702.
- (4) (a) Arevalo, R.; Chirik, P. J. Enabling Two-Electron Pathways with Iron and Cobalt: From Ligand Design to Catalytic Applications. *J. Am. Chem. Soc.* **2019**, *141*, 9106–9123. (b) Karunananda, M. K.; Mankad, N. P. Cooperative Strategies for Catalytic Hydrogenation of Unsaturated Hydrocarbons. *ACS Catal.* **2017**, *7*, 6110–6119. (c) Jacquet, J.; Desage-El Murr, M.; Fensterbank, L. Metal-Promoted Coupling Reactions Implying Ligand-Based Redox Changes. *Chem-CatChem* **2016**, *8*, 3310–3316. (d) Zell, T.; Milstein, D. Hydrogenation and Dehydrogenation Iron Pincer Catalysts Capable of Metal-Ligand Cooperation by Aromatization/Dearomatization. *Acc. Chem. Res.* **2015**, *48*, 1979–1994. (e) Luca, O. R.; Crabtree, R. H. Redox-Active Ligands in Catalysis. *Chem. Soc. Rev.* **2013**, *42*, 1440–1459. (f) Darmon, J. M.; Stieber, S. C. E.; Sylvester, K. T.; Fernández, I.; Lobkovsky, E.; Semproni, S. P.; Bill, E.; Wieghardt, K.; DeBeer, S.; Chirik, P. J. Oxidative Addition of Carbon-Carbon Bonds with a Redox-Active Bis(imino)pyridine Iron Complex. *J. Am. Chem. Soc.* **2012**, *134*, 17125–17137. (g) Lyaskovskyy, V.; de Bruin, B. Redox Non-Innocent Ligands: Versatile New Tools to Control Catalytic Reactions. *ACS Catal.* **2012**, *2*, 270–279.
- (5) (a) Wu, C.; Liao, J.; Ge, S. Cobalt-Catalyzed Enantioselective Hydroboration/Cyclization of 1,7-Enynes: Asymmetric Synthesis of Chiral Quinolinones Containing Quaternary Stereogenic Centers. *Angew. Chem., Int. Ed.* **2019**, *58*, 8882–8886. (b) Wen, H.; Wang, K.; Zhang, Y.; Liu, G.; Huang, Z. Cobalt-Catalyzed Regio- and Enantioselective Markovnikov 1,2-Hydrosilylation of Conjugated Dienes. *ACS Catal.* **2019**, *9*, 1612–1618. (c) Ghosh, C.; Kim, S.;

- Mena, M. R.; Kim, J.-H.; Pal, R.; Rock, C. L.; Groy, T. L.; Baik, M.-H.; Trovitch, R. J. Efficient Cobalt Catalyst for Ambient-Temperature Nitrolysis Dihydroboration, the Elucidation of a Chelate-Assisted Borylation Mechanism, and a New Synthetic Route to Amides. *J. Am. Chem. Soc.* **2019**, *141*, 15327–15337. (d) Espinosa, M. R.; Charboneau, D. J.; Garcia de Oliveira, A.; Hazari, N. Controlling Selectivity in the Hydroboration of Carbon Dioxide to the Formic Acid, Formaldehyde, and Methanol Oxidation Levels. *ACS Catal.* **2019**, *9*, 301–314. (e) Hu, M.-Y.; He, Q.; Fan, S.-J.; Wang, Z.-C.; Liu, L.-Y.; Mu, Y.-J.; Peng, Q.; Zhu, S.-F. Ligands with 1,10-phenanthroline scaffold for highly regioselective iron-catalyzed alkene hydrosilylation. *Nat. Commun.* **2018**, *9*, 221. (f) Friedfeld, M. R.; Zhong, H.; Ruck, R. T.; Shevlin, M.; Chirik, P. J. Cobalt-catalyzed asymmetric hydrogenation of enamides enabled by single-electron reduction. *Science* **2018**, *360*, 888. (g) Wang, C.; Teo, W. J.; Ge, S. Access to stereodefined (Z)-allylsilanes and (Z)-allylic alcohols via cobalt-catalyzed regioselective hydrosilylation of allenes. *Nat. Commun.* **2017**, *8*, 1–9. (h) Hoyt, J. M.; Schmidt, V. A.; Tondreau, A. M.; Chirik, P. J. Iron-catalyzed intermolecular [2 + 2] cycloadditions of unactivated alkenes. *Science* **2015**, *349*, 960. (i) Bleith, T.; Wadepohl, H.; Gade, L. H. Iron Achieves Noble Metal Reactivity and Selectivity: Highly Reactive and Enantioselective Iron Complexes as Catalysts in the Hydrosilylation of Ketones. *J. Am. Chem. Soc.* **2015**, *137*, 2456–2459. (j) Friedfeld, M. R.; Shevlin, M.; Hoyt, J. M.; Kraska, S. W.; Tudge, M. T.; Chirik, P. J. Cobalt Precursors for High-Throughput Discovery of Base Metal Asymmetric Alkene Hydrogenation Catalysts. *Science* **2013**, *342*, 1076. (k) Zuo, W.; Lough, A. J.; Li, Y. F.; Morris, R. H. Amine(imine)diphosphine Iron Catalysts for Asymmetric Transfer Hydrogenation of Ketones and Imines. *Science* **2013**, *342*, 1080. (l) Langer, R.; Leitus, G.; Ben-David, Y.; Milstein, D. Efficient Hydrogenation of Ketones Catalyzed by an Iron Pincer Complex. *Angew. Chem., Int. Ed.* **2011**, *50*, 2120–2124. (m) Langer, R.; Diskin-Posner, Y.; Leitus, G.; Shimon, L. J. W.; Ben-David, Y.; Milstein, D. Low-Pressure Hydrogenation of Carbon Dioxide Catalyzed by an Iron Pincer Complex Exhibiting Noble Metal Activity. *Angew. Chem., Int. Ed.* **2011**, *50*, 9948–9952. (n) Boddien, A.; Mellmann, D.; Gärtner, F.; Jackstell, R.; Junge, H.; Dyson, P. J.; Laurenczy, G.; Ludwig, R.; Beller, M. Efficient Dehydrogenation of Formic Acid Using an Iron Catalyst. *Science* **2011**, *333*, 1733. (o) Federsel, C.; Boddien, A.; Jackstell, R.; Jennerjahn, R.; Dyson, P. J.; Scopelliti, R.; Laurenczy, G.; Beller, M. A Well-Defined Iron Catalyst for the Reduction of Bicarbonates and Carbon Dioxide to Formates, Alkyl Formates, and Formamides. *Angew. Chem., Int. Ed.* **2010**, *49*, 9777–9780. (p) Bart, S. C.; Lobkovsky, E.; Chirik, P. J. Preparation and Molecular and Electronic Structures of Iron(0) Dinitrogen and Silane Complexes and Their Application to Catalytic Hydrogenation and Hydrosilylation. *J. Am. Chem. Soc.* **2004**, *126*, 13794–13807. (q) Nakamura, M.; Matsuo, K.; Ito, S.; Nakamura, E. Iron-Catalyzed Cross-Coupling of Primary and Secondary Alkyl Halides with Aryl Grignard Reagents. *J. Am. Chem. Soc.* **2004**, *126*, 3686–3687.
- (6) (a) Alig, L.; Fritz, M.; Schneider, S. First-Row Transition Metal (De)Hydrogenation Catalysis Based On Functional Pincer Ligands. *Chem. Rev.* **2019**, *119*, 2681–2751. (b) Fritz, M.; Schneider, S. The Renaissance of Base Metal Catalysis Enabled by Functional Ligands. In *The Periodic Table II: Catalytic, Materials, Biological and Medical Applications*; Mingos, D. M. P., Ed.; Springer International Publishing: Cham, Switzerland, 2019; pp 1–36. (c) Gandeepan, P.; Müller, T.; Zell, D.; Cera, G.; Warratz, S.; Ackermann, L. 3d Transition Metals for C-H Activation. *Chem. Rev.* **2019**, *119*, 2192–2452. (d) Du, X.; Huang, Z. Advances in Base-Metal-Catalyzed Alkene Hydrosilylation. *ACS Catal.* **2017**, *7*, 1227–1243.
- (7) (a) Hapke, M.; Hilt, G. *Cobalt Catalysis in Organic Synthesis: Methods and Reactions*; Wiley, 2020. (b) Wen, H.; Liu, G.; Huang, Z. Recent Advances in Tridentate Iron and Cobalt Complexes for Alkene and Alkyne Hydrofunctionalizations. *Coord. Chem. Rev.* **2019**, *386*, 138–153. (c) Junge, K.; Papa, V.; Beller, M. Cobalt-Pincer Complexes in Catalysis. *Chem. - Eur. J.* **2019**, *25*, 122–143. (d) Jones, W. D. Hydrogenation/Dehydrogenation of Unsaturated Bonds with Iron Pincer Catalysis. In *Organometallics for Green Catalysis*; Dixneuf, P. H.; Soullé, J.-F., Eds.; Springer International Publishing: Cham, Switzerland, 2019; pp 141–174. (e) Wei, D.; Darcel, C. Iron Catalysis in Reduction and Hydrometalation Reactions. *Chem. Rev.* **2019**, *119*, 2550–2610. (f) Raya-Barón, Á.; Oña-Burgos, P.; Fernández, I. Iron-Catalyzed Homogeneous Hydrosilylation of Ketones and Aldehydes: Advances and Mechanistic Perspective. *ACS Catal.* **2019**, *9*, 5400–5417. (g) Zell, T.; Langer, R. From Ruthenium to Iron and Manganese—A Mechanistic View on Challenges and Design Principles of Base-Metal Hydrogenation Catalysts. *ChemCatChem* **2018**, *10*, 1930–1940. (h) Mukherjee, A.; Milstein, D. Homogeneous Catalysis by Cobalt and Manganese Pincer Complexes. *ACS Catal.* **2018**, *8*, 11435–11469. (i) Fürstner, A. Iron Catalysis in Organic Synthesis: A Critical Assessment of What It Takes To Make This Base Metal a Multitasking Champion. *ACS Cent. Sci.* **2016**, *2*, 778–789. (j) Sun, J.; Deng, L. Cobalt Complex-Catalyzed Hydrosilylation of Alkenes and Alkynes. *ACS Catal.* **2016**, *6*, 290–300. (k) Bauer, I.; Knölker, H.-J. Iron Catalysis in Organic Synthesis. *Chem. Rev.* **2015**, *115*, 3170–3387. Nakazawa, H.; Itazaki, M. Fe–H Complexes in Catalysis. In *Iron Catalysis: Fundamentals and Applications*; Plietker, B., Ed.; Springer: Berlin, 2011; pp 27–81. (m) Junge, K.; Schroeder, K.; Beller, M. Homogeneous Catalysis using Iron Complexes. Recent Developments in Selective Reductions. *Chem. Commun. (Cambridge, U. K.)* **2011**, *47*, 4849–4859. (n) Sherry, B. D.; Fürstner, A. The Promise and Challenge of Iron-Catalyzed Cross Coupling. *Acc. Chem. Res.* **2008**, *41*, 1500–1511.
- (8) (a) Kallmeier, F.; Kempe, R. Manganese Complexes for (De)Hydrogenation Catalysis: A Comparison to Cobalt and Iron Catalysts. *Angew. Chem., Int. Ed.* **2018**, *57*, 46–60. (b) Yang, X.; Wang, C. Manganese-Catalyzed Hydrosilylation Reactions. *Chem. - Asian J.* **2018**, *13*, 2307–2315. (c) Gorgas, N.; Kirchner, K. Isoelectronic Manganese and Iron Hydrogenation/Dehydrogenation Catalysts: Similarities and Divergences. *Acc. Chem. Res.* **2018**, *51*, 1558–1569. (d) Garbe, M.; Junge, K.; Beller, M. Homogeneous Catalysis by Manganese-Based Pincer Complexes. *Eur. J. Org. Chem.* **2017**, *2017*, 4344–4362. (e) Carney, J. R.; Dillon, B. R.; Thomas, S. P. Recent Advances of Manganese Catalysis for Organic Synthesis. *Eur. J. Org. Chem.* **2016**, *2016*, 3912–3929. (f) Liu, W.; Ackermann, L. Manganese-Catalyzed C-H Activation. *ACS Catal.* **2016**, *6*, 3743–3752. (g) Khusnutdinov, R. I.; Bayguzina, A. R.; Dzhemilev, U. M. Manganese Compounds in the Catalysis of Organic Reactions. *Russ. J. Org. Chem.* **2012**, *48*, 309–348.
- (9) (a) Russell, S. K.; Bowman, A. C.; Lobkovsky, E.; Wieghardt, K.; Chirik, P. J. Synthesis and Electronic Structure of Reduced Bis(imino)pyridine Manganese Compounds. *Eur. J. Inorg. Chem.* **2012**, *2012*, 535–545. (b) Reardon, D.; Aharonian, G.; Gambarotta, S.; Yap, G. P. A. Mono- and Zerovalent Manganese Alkyl Complexes Supported by the α,α' -Diiminato Pyridine Ligand: Alkyl Stabilization at the Expense of Catalytic Performance. *Organometallics* **2002**, *21*, 786–788.
- (10) Please note that, although manganese(I)-based catalysts are more prevalent, both low- and high-spin manganese(II) complexes can be highly active in catalysis. For example, see: Vasilenko, V.; Blasius, C. K.; Gade, L. H. One-Pot Sequential Kinetic Profiling of a Highly Reactive Manganese Catalyst for Ketone Hydroboration: Leveraging σ -Bond Metathesis via Alkoxide Exchange Steps. *J. Am. Chem. Soc.* **2018**, *140*, 9244–9254. Kelly, C. M.; McDonald, R.; Sydora, O. L.; Stradiotto, M.; Turculet, L. A Manganese Pre-Catalyst: Mild Reduction of Amides, Ketones, Aldehydes, and Esters. *Angew. Chem., Int. Ed.* **2017**, *56*, 15901–15904. Mukhopadhyay, T. K.; Flores, M.; Groy, T. L.; Trovitch, R. J. A Highly Active Manganese Precatalyst for the Hydrosilylation of Ketones and Esters. *J. Am. Chem. Soc.* **2014**, *136*, 882–885.
- (11) (a) Chakraborty, S.; Gellrich, U.; Diskin-Posner, Y.; Leitus, G.; Avram, L.; Milstein, D. Manganese-Catalyzed N-Formylation of Amines by Methanol Liberating H₂: A Catalytic and Mechanistic Study. *Angew. Chem., Int. Ed.* **2017**, *56*, 4229–4233. (b) Nerush, A.; Vogt, M.; Gellrich, U.; Leitus, G.; Ben-David, Y.; Milstein, D. Template Catalysis by Metal-Ligand Cooperation. C-C Bond

Formation via Conjugate Addition of Non-activated Nitriles under Mild, Base-free Conditions Catalyzed by a Manganese Pincer Complex. *J. Am. Chem. Soc.* **2016**, *138*, 6985–6997.

(12) (a) Deibl, N.; Kempe, R. Manganese-Catalyzed Multi-component Synthesis of Pyrimidines from Alcohols and Amidines. *Angew. Chem., Int. Ed.* **2017**, *56*, 1663–1666. (b) Kallmeier, F.; Irrgang, T.; Dietel, T.; Kempe, R. Highly Active and Selective Manganese C = O Bond Hydrogenation Catalysts: The Importance of the Multidentate Ligand, the Ancillary Ligands, and the Oxidation State. *Angew. Chem., Int. Ed.* **2016**, *55*, 11806–11809.

(13) (a) Ryabchuk, P.; Stier, K.; Junge, K.; Checinski, M. P.; Beller, M. Molecularly Defined Manganese Catalyst for Low-Temperature Hydrogenation of Carbon Monoxide to Methanol. *J. Am. Chem. Soc.* **2019**, *141*, 16923–16929. (b) Elangovan, S.; Topf, C.; Fischer, S.; Jiao, H.; Spannenberg, A.; Baumann, W.; Ludwig, R.; Junge, K.; Beller, M. Selective Catalytic Hydrogenations of Nitriles, Ketones, and Aldehydes by Well-Defined Manganese Pincer Complexes. *J. Am. Chem. Soc.* **2016**, *138*, 8809–8814.

(14) (a) Weber, S.; Stöger, B.; Veiros, L. F.; Kirchner, K. Rethinking Basic Concepts—Hydrogenation of Alkenes Catalyzed by Bench-Stable Alkyl Mn(I) Complexes. *ACS Catal.* **2019**, *9*, 9715–9720. (b) Mastalir, M.; Glatz, M.; Pittenauer, E.; Allmaier, G.; Kirchner, K. Sustainable Synthesis of Quinolines and Pyrimidines Catalyzed by Manganese PNP Pincer Complexes. *J. Am. Chem. Soc.* **2016**, *138*, 15543–15546.

(15) (a) Erken, C.; Kaithal, A.; Sen, S.; Weyhermüller, T.; Hölscher, M.; Werlé, C.; Leitner, W. Manganese-Catalyzed Hydroboration of Carbon Dioxide and other Challenging Carbonyl Groups. *Nat. Commun.* **2018**, *9*, 4521. (b) Kulkarni, N. V.; Brennessel, W. W.; Jones, W. D. Catalytic Upgrading of Ethanol to n-Butanol via Manganese-Mediated Guerbet Reaction. *ACS Catal.* **2018**, *8*, 997–1002. (c) Widegren, M. B.; Harkness, G. J.; Slawin, A. M. Z.; Cordes, D. B.; Clarke, M. L. A Highly Active Manganese Catalyst for Enantioselective Ketone and Ester Hydrogenation. *Angew. Chem., Int. Ed.* **2017**, *56*, 5825–5828.

(16) (a) Carney, J. R.; Dillon, B. R.; Campbell, L.; Thomas, S. P. Manganese-Catalyzed Hydrofunctionalization of Alkenes. *Angew. Chem., Int. Ed.* **2018**, *57*, 10620–10624. (b) Zhang, G.; Zeng, H.; Wu, J.; Yin, Z.; Zheng, S.; Fettinger, J. C. Highly Selective Hydroboration of Alkenes, Ketones and Aldehydes Catalyzed by a Well-Defined Manganese Complex. *Angew. Chem., Int. Ed.* **2016**, *55*, 14369–14372. (c) Macaulay, C. M.; Gustafson, S. J.; Fuller, J. T.; Kwon, D.-H.; Ogawa, T.; Ferguson, M. J.; McDonald, R.; Lumsden, M. D.; Bischof, S. M.; Sydora, O. L.; Ess, D. H.; Stradiotto, M.; Turculet, L. Alkene Isomerization-Hydroboration Catalyzed by First-Row Transition-Metal (Mn, Fe, Co, and Ni) N-Phosphinoamidinate Complexes: Origin of Reactivity and Selectivity. *ACS Catal.* **2018**, *8*, 9907–9925.

(17) (a) Fernandez, E. *Science of Synthesis: Advances in Organoboron Chemistry Towards Organic Synthesis*; George Thieme Verlag, 2019. (b) Hall, D. G. *Boronic Acids: Preparation and Applications in Organic Synthesis and Medicine*, 1st ed.; Wiley-VCH: Weinheim, Germany, 2005; pp 1–549.

(18) (a) Suzuki, A. Cross-Coupling Reactions Of Organoboranes: An Easy Way To Construct C-C Bonds (Nobel Lecture). *Angew. Chem., Int. Ed.* **2011**, *50*, 6722–6737. (b) Miyaura, N.; Suzuki, A. Palladium-Catalyzed Cross-Coupling Reactions of Organoboron Compounds. *Chem. Rev.* **1995**, *95*, 2457–2483.

(19) (a) Cuenca, A. B.; Fernández, E. Rhodium-Catalyzed C–B Bond Formation. In *Rhodium Catalysis*; Claver, C., Ed.; Springer International Publishing: Cham, Switzerland, 2018; pp 1–29. (b) Fernandez, E.; Segarra, A. M. Iridium-Catalyzed Boron-Addition. In *Iridium Complexes in Organic Synthesis*; Oro, L. A., Claver, C., Eds.; Wiley-VCH: Weinheim, Germany, 2009; pp 173–194. (c) Miyaura, N. Metal-Catalyzed Reactions of Organoboronic Acids and Esters. *Bull. Chem. Soc. Jpn.* **2008**, *81*, 1535–1553. (d) Vogels, C.; Westcott, S. Recent Advances in Organic Synthesis Using Transition Metal-Catalyzed Hydroborations. *Curr. Org. Chem.* **2005**, *9*, 687–699.

(20) (a) Wu, C.; Ge, S. Ligand-Controlled Cobalt-Catalyzed Regiodivergent Hydroboration of Aryl,Alkyl-Disubstituted Internal Alkenes. *Chem. Sci.* **2020**, *11*, 2783. (b) Chen, X.; Cheng, Z.; Lu, Z. Cobalt-Catalyzed Asymmetric Markovnikov Hydroboration of Styrenes. *ACS Catal.* **2019**, *9*, 4025–4029. (c) Huang, Q.; Hu, M.-Y.; Zhu, S.-F. Cobalt-Catalyzed Cyclization/Hydroboration of 1,6-Diynes with Pinacolborane. *Org. Lett.* **2019**, *21*, 7883–7887. (d) Leonard, N. G.; Palmer, W. N.; Friedfeld, M. R.; Bezdek, M. J.; Chirik, P. J. Remote, Diastereoselective Cobalt-Catalyzed Alkene Isomerization-Hydroboration: Access to Stereodefined 1,3-Difunctionalized Indanes. *ACS Catal.* **2019**, *9*, 9034–9044. (e) Cruz, T. F. C.; Lopes, P. S.; Pereira, L. C. J.; Veiros, L. F.; Gomes, P. T. Hydroboration of Terminal Olefins with Pinacolborane Catalyzed by New Mono(2-Iminopyrrolyl) Cobalt(II) Complexes. *Inorg. Chem.* **2018**, *57*, 8146–8159. (f) Zuo, Z.; Wen, H.; Liu, G.; Huang, Z. Cobalt-Catalyzed Hydroboration and Borylation of Alkenes and Alkynes. *Synlett* **2018**, *29*, 1421–1429. (g) Cruz, T. F. C.; Veiros, L. F.; Gomes, P. T. Cobalt(I) Complexes of 5-Aryl-2-iminopyrrolyl Ligands: Synthesis, Spin Isomerism, and Application in Catalytic Hydroboration. *Inorg. Chem.* **2018**, *57*, 14671–14685. (h) Tamang, S. R.; Bedi, D.; Shafiei-Haghighi, S.; Smith, C. R.; Crawford, C.; Findlater, M. Cobalt-Catalyzed Hydroboration of Alkenes, Aldehydes, and Ketones. *Org. Lett.* **2018**, *20*, 6695–6700. (i) Bai, T.; Janes, T.; Song, D. Homoleptic Iron(II) and Cobalt(II) Bis(Phosphoramidate) Complexes for the Selective Hydrofunctionalization of Unsaturated Molecules. *Dalton Trans.* **2017**, *46*, 12408–12412. (j) Zhang, G.; Wu, J.; Wang, M.; Zeng, H.; Cheng, J.; Neary, M. C.; Zheng, S. Cobalt-Catalyzed Regioselective Hydroboration of Terminal Alkenes. *Eur. J. Org. Chem.* **2017**, *2017*, 5814–5818. (k) Peng, J.; Docherty, J. H.; Dominey, A. P.; Thomas, S. P. Cobalt-Catalyzed Markovnikov Selective Hydroboration of Vinylarenes. *Chem. Commun.* **2017**, *53*, 4726–4729. (l) Chu, W.-Y.; Gilbert-Wilson, R.; Rauchfuss, T. B.; van Gestel, M.; Neese, F. Cobalt Phosphino- α -Iminopyridine-Catalyzed Hydrofunctionalization of Alkenes: Catalyst Development and Mechanistic Analysis. *Organometallics* **2016**, *35*, 2900–2914. (m) Ibrahim, A. D.; Entsminger, S. W.; Zhu, L.; Fout, A. R. A Highly Chemoselective Cobalt Catalyst for the Hydrosilylation of Alkenes using Tertiary Silanes and Hydrosiloxanes. *ACS Catal.* **2016**, *6*, 3589–3593. (n) Palmer, W. N.; Diao, T.; Pappas, I.; Chirik, P. J. High-Activity Cobalt Catalysts for Alkene Hydroboration with Electronically Responsive Terpyridine and α -Diimine Ligands. *ACS Catal.* **2015**, *5*, 622–626. (o) Scheuermann, M. L.; Johnson, E. J.; Chirik, P. J. Alkene Isomerization-Hydroboration Promoted by Phosphine-Ligated Cobalt Catalysts. *Org. Lett.* **2015**, *17*, 2716–2719. (p) Ruddy, A. J.; Sydora, O. L.; Small, B. L.; Stradiotto, M.; Turculet, L. (N-Phosphinoamidinate)Cobalt-Catalyzed Hydroboration: Alkene Isomerization Affords Terminal Selectivity. *Chem. - Eur. J.* **2014**, *20*, 13918–13922. (q) Obligacion, J. V.; Chirik, P. J. Bis(imino)pyridine Cobalt-Catalyzed Alkene Isomerization-Hydroboration: A Strategy for Remote Hydrofunctionalization with Terminal Selectivity. *J. Am. Chem. Soc.* **2013**, *135*, 19107–19110.

(21) (a) Su, W.; Qiao, R.-X.; Zhen, X.-L.; Tian, X.; Han, J.-R.; Fan, S.-M.; Cheng, Q.-S.; Liu, S.-X. Ligand-Free Iron-Catalyzed Regiodivergent Hydroboration of Unactivated Terminal Alkenes. *Chem.Rxiv* **2020**, 1–7. (b) Chen, X.; Cheng, Z.; Lu, Z. Iron-Catalyzed, Markovnikov-Selective Hydroboration of Styrenes. *Org. Lett.* **2017**, *19*, 969–971. (c) Ogawa, T.; Ruddy, A. J.; Sydora, O. L.; Stradiotto, M.; Turculet, L. Cobalt- and Iron-Catalyzed Isomerization-Hydroboration of Branched Alkenes: Terminal Hydroboration with Pinacolborane and 1,3,2-Diazaborolanes. *Organometallics* **2017**, *36*, 417–423. (d) Espinal-Viguri, M.; Woof, C. R.; Webster, R. L. Iron-Catalyzed Hydroboration: Unlocking Reactivity through Ligand Modulation. *Chem. - Eur. J.* **2016**, *22*, 11605–11608. (e) MacNair, A. J.; Millet, C. R. P.; Nichol, G. S.; Ironmonger, A.; Thomas, S. P. Markovnikov-Selective, Activator-Free Iron-Catalyzed Vinylarene Hydroboration. *ACS Catal.* **2016**, *6*, 7217–7221. (f) Greenhalgh, M. D.; Jones, A. S.; Thomas, S. P. Iron-Catalyzed Hydrofunctionalisation of Alkenes and Alkynes. *ChemCatChem* **2015**, *7*, 190–222. (g) Obligacion, J. V.; Chirik, P. J. Highly Selective

- Bis(imino)pyridine Iron-Catalyzed Alkene Hydroboration. *Org. Lett.* **2013**, *15*, 2680–2683. (h) Zhang, L.; Huang, Z. Iron-Catalyzed Alkene Hydroboration with Pinacolborane. *Synlett* **2013**, *24*, 1745–1747. (i) Zhang, L.; Peng, D.; Leng, X.; Huang, Z. Iron-Catalyzed, Atom-Economical, Chemo- and Regioselective Alkene Hydroboration with Pinacolborane. *Angew. Chem., Int. Ed.* **2013**, *52*, 3676–3680. (j) Wu, J. Y.; Moreau, B.; Ritter, T. Iron-Catalyzed 1,4-Hydroboration of 1,3-Dienes. *J. Am. Chem. Soc.* **2009**, *131*, 12915–12917.
- (22) (a) Touney, E. E.; Van Hoveln, R.; Buttke, C. T.; Freidberg, M. D.; Guzei, I. A.; Schomaker, J. M. Heteroleptic Nickel Complexes for the Markovnikov-Selective Hydroboration of Styrenes. *Organometallics* **2016**, *35*, 3436–3439. (b) Ulm, F.; Chetcuti, M. J.; Ritleng, V.; Cornaton, Y.; Djukic, J.-P. Hydroboration of alkenes catalysed by a nickel N-heterocyclic carbene complex: reaction and mechanistic aspects. *Chem. - Eur. J.* **2020**, *26*, 8916–8925. (c) Vijaykumar, G.; Bhunia, M.; Mandal, S. K. A phenalenyl-based nickel catalyst for the hydroboration of olefins under ambient conditions. *Dalton Trans.* **2019**, *48*, 5779–5784. (d) Li, J.-F.; Wei, Z.-Z.; Wang, Y.-Q.; Ye, M. Base-free nickel-catalyzed hydroboration of simple alkenes with bis(pinacolato)diboron in an alcoholic solvent. *Green Chem.* **2017**, *19*, 4498–4502.
- (23) (a) Iwamoto, H.; Iwamoto, T.; Ito, H. Computational design of high-performance ligand for enantioselective Markovnikov hydroboration of aliphatic terminal alkenes. *Nat. Commun.* **2018**, *9*, 2290. (b) Lee, Y.; Hoveyda, A. H. Efficient Boron-Copper Additions to Aryl-Substituted Alkenes Promoted by NHC-Based Catalysts. Enantioselective Cu-Catalyzed Hydroboration Reactions. *J. Am. Chem. Soc.* **2009**, *131*, 3160–3161. (c) Semba, K.; Fujihara, T.; Terao, J.; Tsuji, Y. Copper-catalyzed borylative transformations of non-polar carbon-carbon unsaturated compounds employing borylcopper as an active catalyst species. *Tetrahedron* **2015**, *71*, 2183–2197. (d) Noh, D.; Chea, H.; Ju, J.; Yun, J. Highly Regio- and Enantioselective Copper-Catalyzed Hydroboration of Styrenes. *Angew. Chem., Int. Ed.* **2009**, *48*, 6062–6064.
- (24) (a) Tamang, S. R.; Findlater, M. Emergence and Applications of Base Metals (Fe, Co, and Ni) in Hydroboration and Hydrosilylation. *Molecules* **2019**, *24*, 3194. (b) Obligacion, J. V.; Chirik, P. J. Earth-Abundant Transition Metal Catalysts for Alkene Hydrosilylation and Hydroboration. *Nat. Rev. Chem.* **2018**, *2*, 15–34.
- (25) Sommer, H.; Juliá-Hernández, F.; Martin, R.; Marek, I. Walking Metals for Remote Functionalization. *ACS Cent. Sci.* **2018**, *4*, 153–165.
- (26) (a) Lu, C. C.; Bill, E.; Weyhermüller, T.; Bothe, E.; Wieghardt, K. Neutral Bis(α -iminopyridine)metal Complexes of the First-Row Transition Ions (Cr, Mn, Fe, Co, Ni, Zn) and Their Monocationic Analogues: Mixed Valency Involving a Redox Noninnocent Ligand System. *J. Am. Chem. Soc.* **2008**, *130*, 3181–3197. (b) Bart, S. C.; Chlopek, K.; Bill, E.; Bouwkamp, M. W.; Lobkovsky, E.; Neese, F.; Wieghardt, K.; Chirik, P. J. Electronic Structure of Bis(imino)pyridine Iron Dichloride, Monochloride, and Neutral Ligand Complexes: A Combined Structural, Spectroscopic, and Computational Study. *J. Am. Chem. Soc.* **2006**, *128*, 13901–13912.
- (27) (a) Mukhopadhyay, T. K.; Flores, M.; Groy, T. L.; Trovitch, R. J. A Highly Active Manganese Precatalyst for the Hydrosilylation of Ketones and Esters. *J. Am. Chem. Soc.* **2014**, *136*, 882–885. (b) Paris, S. I. M.; Laskay, Ü. A.; Liang, S.; Pavlyuk, O.; Tschirschwitz, S.; Lönnecke, P.; McMills, M. C.; Jackson, G. P.; Petersen, J. L.; Hey-Hawkins, E.; Jensen, M. P. Manganese(II) Complexes of Di-2-pyridinylmethylene-1,2-diimine Di-Schiff Base Ligands: Structures And Reactivity. *Inorg. Chim. Acta* **2010**, *363*, 3390–3398. (c) Ebralidze, I. I.; Leitus, G.; Shimon, L. J. W.; Wang, Y.; Shaik, S.; Neumann, R. Structural Variability in Manganese(II) Complexes of N,N'-Bis(2-pyridinylmethylene) Ethane (and Propane) Diamine Ligands. *Inorg. Chim. Acta* **2009**, *362*, 4713–4720. (d) Figgs, B. N.; Lewis, J. The Magnetic Properties of Transition Metal Complexes. In *Progress in Inorganic Chemistry*; Cotton, F. A., Ed.; Wiley-VCH, 2007; pp 37–239.
- (28) (a) Gusev, A.; Nemeč, I.; Herchel, R.; Riush, I.; Titiš, J.; Boča, R.; Lyssenko, K.; Kiskin, M.; Eremenko, I.; Linert, W. Structural and Magnetic Characterization of Ni(II), Co(II), and Fe(II) Binuclear Complexes on a Bis(Pyridyl-Triazolyl)Alkane Basis. *Dalton Trans.* **2019**, *48*, 10526–10536. (b) Herchel, R.; Váhovská, L.; Potočňák, I.; Trávníček, Z. Slow Magnetic Relaxation in Octahedral Cobalt(II) Field-Induced Single-Ion Magnet with Positive Axial and Large Rhombic Anisotropy. *Inorg. Chem.* **2014**, *53*, 5896–5898. (c) Mishra, V.; Lloret, F.; Mukherjee, R. Coordination Versatility of 1,3-bis[3-(2-pyridyl)pyrazol-1-yl]propane: Co(II) and Ni(II) Complexes. *Inorg. Chim. Acta* **2006**, *359*, 4053–4062. (d) Chen, L.; Albert Cotton, F. Cobalt(II) Complexes with the 1,5,9,13-Tetraazacyclohexadecane Ligand. *Inorg. Chim. Acta* **1997**, *263*, 9–16.
- (29) Docherty, J. H.; Peng, J.; Dominey, A. P.; Thomas, S. P. Activation and Discovery of Earth-Abundant Metal Catalysts Using Sodium Tert-Butoxide. *Nat. Chem.* **2017**, *9*, 595–600.
- (30) Bage, A. D.; Hunt, T. A.; Thomas, S. P. Hidden Boron Catalysis: Nucleophile-Promoted Decomposition of HBpin. *Org. Lett.* **2020**, *22*, 4107–4112.
- (31) Considering computational cost, we use catalyst model systems in which the isopropyl substituents on the imine are replaced with methyl substituents. For full computational details, see the [Supporting Information](#).
- (32) Griffith, G. A.; Al-Khatib, M. J.; Patel, K.; Singh, K.; Solan, G. A. Solid and Solution State Flexibility of Sterically Congested Bis(imino)bipyridine Complexes of Zinc(II) and Nickel(II). *Dalton Trans.* **2009**, 185–196.
- (33) We note that we could not locate equilibrium structures for the quintet metal hydride species. Because our subsequent investigation of the reaction mechanism returned transition structures with inaccessibly high energies, we will not further consider the quintet PES. (Absolute energies and geometries of the transition structures are given in the [Supporting Information](#).)
- (34) (a) Chirik, P. J. Electronic Structures of Reduced Manganese, Iron, and Cobalt Complexes Bearing Redox-Active Bis(imino)pyridine Pincer Ligands. In *Pincer and Pincer-Type Complexes: Applications in Organic Synthesis and Catalysis*; Szabo, K. J., Wendt, O. F., Eds.; Wiley-VCH: Weinheim, Germany, 2014; pp 189–212. (b) Zhou, Y.-Y.; Hartline, D. R.; Steiman, T. J.; Fanwick, P. E.; Uyeda, C. Dinuclear Nickel Complexes in Five States of Oxidation Using a Redox-Active Ligand. *Inorg. Chem.* **2014**, *53*, 11770–11777. (c) Lu, C. C.; Weyhermüller, T.; Bill, E.; Wieghardt, K. Accessing the Different Redox States of α -Iminopyridines within Cobalt Complexes. *Inorg. Chem.* **2009**, *48*, 6055–6064. (d) de Bruin, B.; Bill, E.; Bothe, E.; Weyhermüller, T.; Wieghardt, K. Molecular and Electronic Structures of Bis(pyridine-2,6-diimine)metal Complexes $[ML_2](PF_6)_n$ ($n = 0, 1, 2, 3$; $M = Mn, Fe, Co, Ni, Cu, Zn$). *Inorg. Chem.* **2000**, *39*, 2936–2947.
- (35) The singlet state, although possible, has exceedingly high barriers for migratory insertion ([Tables S6 and S7](#)) and was not considered any further.
- (36) For a comparison between cobalt and manganese complexes with pyridinediimine ligands, see: Obligacion, J. V.; Chirik, P. J. bis(imino)pyridine Cobalt-Catalyzed Alkene Isomerization-Hydroboration: A Strategy for Remote Hydrofunctionalization with Terminal Selectivity. *J. Am. Chem. Soc.* **2013**, *135*, 19107–19110. Carney, J. R.; Dillon, B. R.; Campbell, L.; Thomas, S. P. Manganese-Catalyzed Hydrofunctionalization of Alkenes. *Angew. Chem., Int. Ed.* **2018**, *57*, 10620–10624.